Lara A. Thompson[1]
Mem. ASME
Biomedical Engineering Program,
School of Engineering and Applied Sciences,
Department of Mechanical Engineering,
University of the District of Columbia,
4200 Connecticut Avenue NW,
Washington, DC 20008;
Harvard-MIT Division of Health
Sciences and Technology,
Massachusetts Institute of Technology,
77 Massachusetts Avenue,
Cambridge, MA 02138
e-mail: lthomps@alum.mit.edu

Csilla Haburcakova
Jenks Vestibular Physiology Laboratory,
Massachusetts Eye and Ear Infirmary,
Boston, MA 02139
e-mail: Csilla_Haburcakova@meei.harvard.edu

Adam D. Goodworth
Department of Rehabilitation Sciences,
University of Hartford,
West Hartford, CT 06117
e-mail: goodworth@hartford.edu

Richard F. Lewis
Departments of Otology and
Laryngology and Neurology,
Harvard Medical School,
Boston, MA 02139;
Jenks Vestibular Physiology Laboratory,
Massachusetts Eye and Ear Infirmary,
Boston, MA 02139
e-mail: richard_lewis@meei.harvard.edu

An Engineering Model to Test for Sensory Reweighting: Nonhuman Primates Serve as a Model for Human Postural Control and Vestibular Dysfunction

Quantitative animal models are critically needed to provide proof of concept for the investigation of rehabilitative balance therapies (e.g., invasive vestibular prostheses) and treatment response prior to, or in conjunction with, human clinical trials. This paper describes a novel approach to modeling the nonhuman primate postural control system. Our observation that rhesus macaques and humans have even remotely similar postural control motivates the further application of the rhesus macaque as a model for studying the effects of vestibular dysfunction, as well as vestibular prosthesis-assisted states, on human postural control. Previously, system identification methodologies and models were only used to describe human posture. However, here we utilized pseudorandom, roll-tilt balance platform stimuli to perturb the posture of a rhesus monkey in normal and mild vestibular (equilibrium) loss states. The relationship between rhesus monkey trunk sway and platform roll-tilt was determined via stimulus–response curves and transfer function results. A feedback controller model was then used to explore sensory reweighting (i.e., changes in sensory reliance), which prevented the animal from falling off of the tilting platform. Conclusions involving sensory reweighting in the nonhuman primate for a normal sensory state and a state of mild vestibular loss led to meaningful insights. This first-phase effort to model the balance control system in nonhuman primates is essential for future investigations toward the effects of invasive rehabilitative (balance) technologies on postural control in primates, and ultimately, humans. [DOI: 10.1115/1.4038157]

Keywords: vestibular loss, pseudorandom stimulus, balance, posture, feedback controller, sensory reweighting

Introduction

Postural Imbalance Leading to Falls Is a Major Concern. For vestibular loss sufferers, elderly individuals, and many others, postural imbalance leading to falls is a major concern. It is estimated that 90 million Americans (approximately 42% of the current population) experience dizziness at least once in their lifetime and, unfortunately, some of these patients will remain with permanent balance deficits [1]. For patients over 75 years of age, dizziness is the number one reason for visiting a physician, and it often leads to increased fall risk in elderly individuals. Falls are a major concern in that they account for 50% of accidental deaths in the elderly; some estimates state that as many of half of all cases of dizziness are due to vestibular disorders, and that those with symptomatic vestibular dysfunction have a 12-fold increase in the odds of falling [2]. Further, approximately 8 million American adults suffer from chronic balance disorders specifically derived from severe peripheral vestibular dysfunction [3] and nearly 3.3 million (i.e., 1 in 20) U.S. children have dizziness and balance problems [4].

The Effects of Vestibular Dysfunction and the Need for Rehabilitative Solutions. Unfortunately, severe vestibular loss sufferers are receiving reduced sensory information necessary to maintain their balance [5,6]. The seemingly simple task of standing involves complex interactions of the sensorimotor system (i.e., the integration of inputs to the visual, somatosensory, and vestibular systems). When healthy individuals are subjected to balance perturbations encountered in daily-living situations (e.g., getting out of bed at night, standing on a moving bus, remaining stable on a tilting platform, or even walking on an uneven surface in the dark), they are able to maintain their balance with little, if any, conscious thought. However, for these common balance situations, individuals suffering from severe vestibular dysfunction have loss of equilibrium that can cause unsteady balance leading to fall-related, debilitating injuries. Although imbalance is a major concern, little is known regarding compensation mechanisms and rehabilitative treatments to aid individuals suffering from vestibular impairments.

Rehabilitative solutions are critically needed to aid individuals suffering from moderate to severe vestibular loss. The testing of rehabilitative solutions, in particular invasive rehabilitative solutions (e.g., vestibular prostheses) which have had limited testing in humans, must be determined in nonhuman primates as a precursor or in parallel [7]. The development of such knowledge base in nonhuman primates can potentially decrease the risks of falling and enhance the benefits associated with future implementation of invasive prostheses in humans. However, a critical component to posture research conducted in primates is first bridging its relevance and applicability to humans (e.g., via use of similar, overarching system identification techniques).

[1]Corresponding author.
Manuscript received December 21, 2016; final manuscript received September 14, 2017; published online October 31, 2017. Assoc. Editor: Beth A. Winkelstein.

Relevant Previous Studies of Human and Animal Postural Control: Important Findings and Limitations. Changes in sensory reliance are essential to maintaining balance in that they prevent humans and animals from falling off of an unstable, tilting surface. Previously, a white noise approximated signal (e.g., pseudorandom ternary sequence (PRTS) stimulus) has been used as a platform tilt input perturbation stimulus for normal and severe vestibular-loss human subjects (e.g., Refs. [8–10]). As the platform surface tilts, proprioceptive cues tend to orient one's body toward the tilted surface while graviceptive cues tend to orient one's body toward earth vertical. As first shown in Ref. [10], unimpaired (normal) humans' root-mean-square (RMS), center-of-mass (COM) body sway saturated as platform tilt amplitude increased (sway saturation). This sway saturation prevented normal humans from falling off of the platform. The sensory reweighting hypothesis states that the normal human "weights" (or relies upon) graviceptive cues more heavily (e.g., vestibular feedback that orients toward earth-vertical) on a tilting support surface (SS), and less so on proprioceptive cues, as the SS amplitude increases. However, human subjects with severe bilateral vestibular loss did not exhibit sway saturation in that their stimulus–response curves remained linear thereby leading to falls at the higher stimulus amplitudes; even at the larger stimulus amplitudes, the severe vestibular-loss subjects continued to orient toward the platform surface and therefore could not maintain their balance.

A feedback controller model has also been used in conjunction with empirical human results (as first shown in Ref. [10]) to test the sensory reweighting hypothesis. Model parameters representing sensory weights varied across stimulus amplitude in a manner consistent with sensory reweighting: as the stimulus amplitude increased, the normal human relied upon (weighted) graviceptive cues more heavily and oriented more with earth-vertical (and less so on proprioceptive cues orienting them with the platform support surface). This change in sensory reliance prevented the normal human from falling off of the platform as tilt amplitude increased. However, the same reweighting was not present in severe bilateral vestibular loss humans, and thus, led to falls at the larger platform tilts.

Although system identification and feedback control have been employed to study human balance with the body represented as a single link inverted pendulum controlled by a proportional-integral-derivative controller (e.g., Refs. [11–16]), very little (if any) has been published on applying these models to predict and characterize postural control nonhuman primate animal subjects. Quantitative animal models are needed to capture the neurophysiological and biomechanical effects of balance disorders, as well as responses to novel rehabilitative solutions that cannot yet be conducted in humans.

Previous quadrupedal posture studies allow for limited comparison to human posture and have not included quantitative posture models. Of the animal, studies which implemented platform tilt inputs to perturb posture, only ramp and hold rotations [16] and discrete sinusoidal inputs (e.g., Refs. [17] and [18]) to the balance platform have been used. Ramp and hold, pitch and roll rotations (for 6 deg peak) of the support surface have been used to study normal and bilateral labyrinthectomized (severe vestibular dysfunction) cats [16]. In the normal animals, there was activation of the extensors of the "uphill" (away from the direction of platform rotation) limbs and inhibition of extensors in the "downhill" (with the direction of platform rotation) limbs. However, following labyrinthectomy, there was an opposite postural response: excitation of the uphill limbs and inhibition of the downhill limbs. This postural response accelerated the body's COM with the downhill rotation, or in the same direction as the platform surface, leading to imbalance and falls. This finding suggested that muscle activation patterns were opposite those of the normal subjects (i.e., abnormal response magnifies body sway leading to destabilization). Although this result showed some consistency with findings in severe bilateral vestibular-loss humans (larger body sway in response to larger stimulus amplitudes [10]), the study was limited in that only static (ramp-hold) platform tilts were used. Furthermore, the methodology previously used did not allow for transfer function modeling which would: (1) facilitate further interpretation of the responses and (2) allow for a more direct and relevant link to human findings (in particular for cutting-edge balance prosthesis research experiments not yet conducted in humans). Further, previous studies did not investigate less marked (mild) vestibular loss cases and implications; changes in sensory reliance for different levels of vestibular impairment were not addressed in human nor animal studies.

Rhesus Monkeys as Models of Human Postural Control. In our study presented here, we hypothesized that the methodology and modeling techniques previously only applied to human studies could be applied to primate test subjects and be used to characterize even more subtle changes in vestibular function (i.e., normal function versus mild vestibular hypofunction (mBVH)). We implemented a white noise approximated platform roll-tilt input stimulus and a sensory integration feedback controller, previously only used to study human postural control, to determine if such techniques and models could be applied to characterize the bipedal hindtrunk of the animal. Further, because the impairment was mild as opposed to severe, this allowed us to test the sensitivity of such a model, which had only been applied to normal and severe (extreme) vestibular dysfunction humans.

The main goals of this study were: (1) to determine if the rhesus monkey stimulus–response curves exhibited sway saturation for normal and/or mBVH sensory states (indicative of a sensory reweighting similar to humans), (2) to describe the rhesus monkey postural control system in terms of system transfer functions (a method previously only used for human posture data), and (3) to determine if feedback control model parameters could describe animal (such as monkey) postural responses, in particular, to test the sensory reweighting hypothesis for the animal in the normal and mBVH states.

We observed that the normal monkey's hindtrunk stimulus–response and transfer results showed characteristics similar to those seen in humans. Specifically, (hindtrunk) sway saturation for increasing stimulus amplitude was observed and feedback model parameters showed that sensory reweighting was present. Our results form the baseline for future posture studies and motivate further application of the rhesus macaque as a model for studying vestibular dysfunction's effects on human postural control.

Methods

Nonhuman Primate Training and Data Collection. All experiments were conducted with the approval of the Massachusetts Eye and Ear Infirmary Institutional Animal Care and Use Committee and were in accordance with USDA guidelines. One adult, female rhesus monkey (5 years, ~6.7 kg) was observed in the normal and mildly vestibular impaired states to collect the empirical data needed to test our model. While in the normal state, the animal was trained to stand free of restraint on a balance platform to receive a juice reward. Once the animal was able to stand on the moving platform, normal (unimpaired) data were collected. After the experiments in the normal state were conducted, the monkey underwent a series of ototoxic treatments to target and kill the vestibular hair cells (described in the Inducing Mild Vestibular Loss section).

A platform-mounted juice reward system with a flexible mouthpiece was used to motivate the animal to stand on the moving platform in its natural quadrupedal stance. Because the reward system was mounted to the platform, its orientation relative to the moving platform did not provide the animal an earth-vertical stationary reference. In order to limit the animal's visual cues, a black tarp surround and dim lighting were used. In the transverse (mediolateral) dimension, the stance width was smaller (9 cm)

than in the longitudinal (anterior–posterior) direction (31 cm). Thus, maintaining balance in the mediolateral direction was a more demanding postural task than in the anterior–posterior direction. As such, the platform was made to move along the roll-axis. To measure the motion of the foretrunk, and hindtrunk, tridirectional angular position, and linear position data were sampled at a rate of 150 Hz (miniBIRD, Ascension Technology Corporation, Milton, VT).

In both the training and testing of the animal, the pseudorandom stimulus used (described below) was presented at roll-tilt amplitudes of 0.5, 1, 2, 4, 6, 8 deg peak-to-peak (or "pp"). The stimulus presentation continued until the monkey stopped attending to the task (e.g., the animal was no longer motivated by the juice reward). Data were collected over multiple days. Depending on the animal's willingness to perform the task, test sessions ranged from a few minutes to 10–15 min. The nature of the pseudorandom, white-noise stimulus is that it is unpredictable to the test subject. Eight cycles were presented at each of the 6 stimulus amplitudes in random fashion. Our goal was to obtain close to 20 usable cycles per stimulus amplitude. In human studies, data were acquired for far fewer cycles per stimulus amplitude, but then averaged across test subjects. Instead, here we obtained close to 20 usable cycles per stimulus amplitude, but then averaged them within a single test subject.

Inducing Mild Vestibular Loss. Vestibular ablation of the animal was accomplished by intratympanic (IT) gentamicin and systemic intramuscular streptomycin injections. Intratympanic gentamicin (IT gent) kills vestibular hair cells and has been used to treat vertigo in Meniere's patients. The monkey received six cycles of bilateral IT gentamicin (350 mg/kg/day for 21 days) followed by 3 cycles of intramuscular streptomycin using the same dosage. The degree of vestibular impairment was quantified in terms of the angular vestibuloocular reflex (VOR) gain (eye velocity/head velocity). The angular VOR, a simple eye movement reflex used to measure semicircular canal function, was tested at discrete frequencies. Final VOR gain (post ablative procedures) was 15% reduction from normal (for 0.1–0.4 Hz). This level of vestibular dysfunction defined the mBVH sensory state.

Pseudorandom Ternary Sequence Roll-Tilt Stimulus. A white noise approximated signal (e.g., PRTS stimulus) has been used as an input perturbation stimulus for human normal and vestibular-loss subjects (e.g., Refs. [8–10], and [12]). However, previous posture studies in animals, other than humans, have not utilized pseudorandom platform-tilt stimuli. This, perhaps, is potentially due to the difficulty of having the animal perform the task while freely standing on the balance platform. Yet it remains that such stimuli are critically invaluable in characterizing an animal's posture in that they are unpredictable to the animal, their duration can be customized to accommodate attention/behavioral focus in animals, and also allow for a bandwidth of frequencies to be tested simultaneously. Further, they allow for the determination of the impulse response, or the system transfer function, which completely characterizes the linear approximated system. Complete details of the PRTS stimulus generation are found within the Appendix. The animal tolerated a shift time of 200 ms, which yielded a cycle period of 16 s and a frequency bandwidth of 0.0625 to ~2.33 Hz.

Figure 1 shows a descriptive schematic with the pseudorandom ternary sequence, or PRTS, (depicted in Fig. 1(*a*)) generated using a shift register and consists of three output states: 0, 1, and 2. In applying a PRTS input stimulus to the balance platform, 0 corresponded to negative platform velocity (or "$-v$"), 1 corresponded to zero platform velocity, and two corresponded to positive platform velocity (or "$+v$") (Fig. 1(*b*)). This was integrated to yield platform stimulus position (Fig. 1(*c*)), and 1(*d*) shows an example of measured (output) trunk position.

Usable Data. In order to identify sections in the normal and mBVH data with human handling artifact, video screening was conducted. Measurements made during PRTS cycles with human handling artifacts and during first cycles of each set of PRTS stimuli were discarded. For all the remaining cycles, offset was removed for each individual cycle. Measurements from remaining cycles for a given stimulus amplitude were pooled and the sample minimum, lower quartile (Q1), median (Q2), upper quartile (Q3), and sample maximum were determined. Outlier sections were defined as those with foretrunk RMS roll less than or greater than Q1-1.5 × (Q3–Q1) and Q3 + 1.5 × (Q3–Q1), respectively [19]. Outlier cycles were identified and discarded from the analysis. The remaining cycles were marked as "usable." A large number of usable cycles were obtained (normal: 18 usable, with roughly 3 unusable cycles per amplitude; mBVH: 23 usable with roughly four unusable cycles per amplitude). Since there was only one test subject, there was no data averaging across various test subjects, as typically done for human studies. Instead, multiple usable PRTS cycles for each stimulus amplitude from one animal were averaged. *T*-tests were used to test for significant differences between the empirical data for the normal and mBVH states' hindtrunk responses. For the model-fitted transfer functions, we used error and normalized-mean-square-error (NMSE) (described further below) to compare empirical and model data.

Nonhuman Primate Empirical Transfer Function Analysis. For a system approximated as linear, cross-correlating a random input signal with the system output response yields an impulse response function, or in the frequency domain the system transfer function that fully characterizes the system. From the measured trunk responses, the frequency response (or system transfer function), as well as trunk orientation as a function of stimulus amplitude (i.e., foretrunk and hindtrunk stimulus–response curves), was determined. The system transfer function, the relationship between output trunk roll to input platform roll, were computed for the normal and mBVH states.

Power spectra were computed and averaged over the number of usable cycles. A discrete Fourier transform (DFT) was used to decompose the PRTS and measured response to their sinusoidal components. The power spectra computed were the following from Eqs. (1)–(3). Within these equations: N are the number of usable cycles, ω is angular frequency, $X_i(j\omega)$ is DFT of the stimulus, $Y_i(j\omega)$ is the discrete Fourier transform of the response, $G_x(j\omega)$ is the power spectral density of the input stimulus, $G_y(j\omega)$ is the power spectral density of the output response, and $G_{xy}(j\omega)$ is the cross power spectral density

$$G_x(j\omega) = \frac{1}{N}\sum_{i=1}^{N} X_i(j\omega)^* \cdot X_i(j\omega) \tag{1}$$

$$G_y(j\omega) = \frac{1}{N}\sum_{i=1}^{N} Y_i(j\omega)^* \cdot Y_i(j\omega) \tag{2}$$

$$G_{xy}(j\omega) = \frac{1}{N}\sum_{i=1}^{N} X_i(j\omega)^* \cdot Y_i(j\omega) \tag{3}$$

A property of the PRTS stimulus is that all even frequency components have zero amplitude [20]. These even frequency points were discarded from the analysis leaving 32 odd frequency samples. Spectra were smoothed by averaging the adjacent frequency points as frequency increased (as described in Ref. [10]). Thus, the power spectra were represented by 12 points. The empirical transfer function, $H(j\omega)$ or tf_{exp}, in Eq. (4) was computed from the smoothed (denoted by the subscript "s") odd frequency bands

$$tf_{\text{exp}} = H(j\omega) = \frac{G_{xys}(j\omega)}{G_{xs}(j\omega)} \tag{4}$$

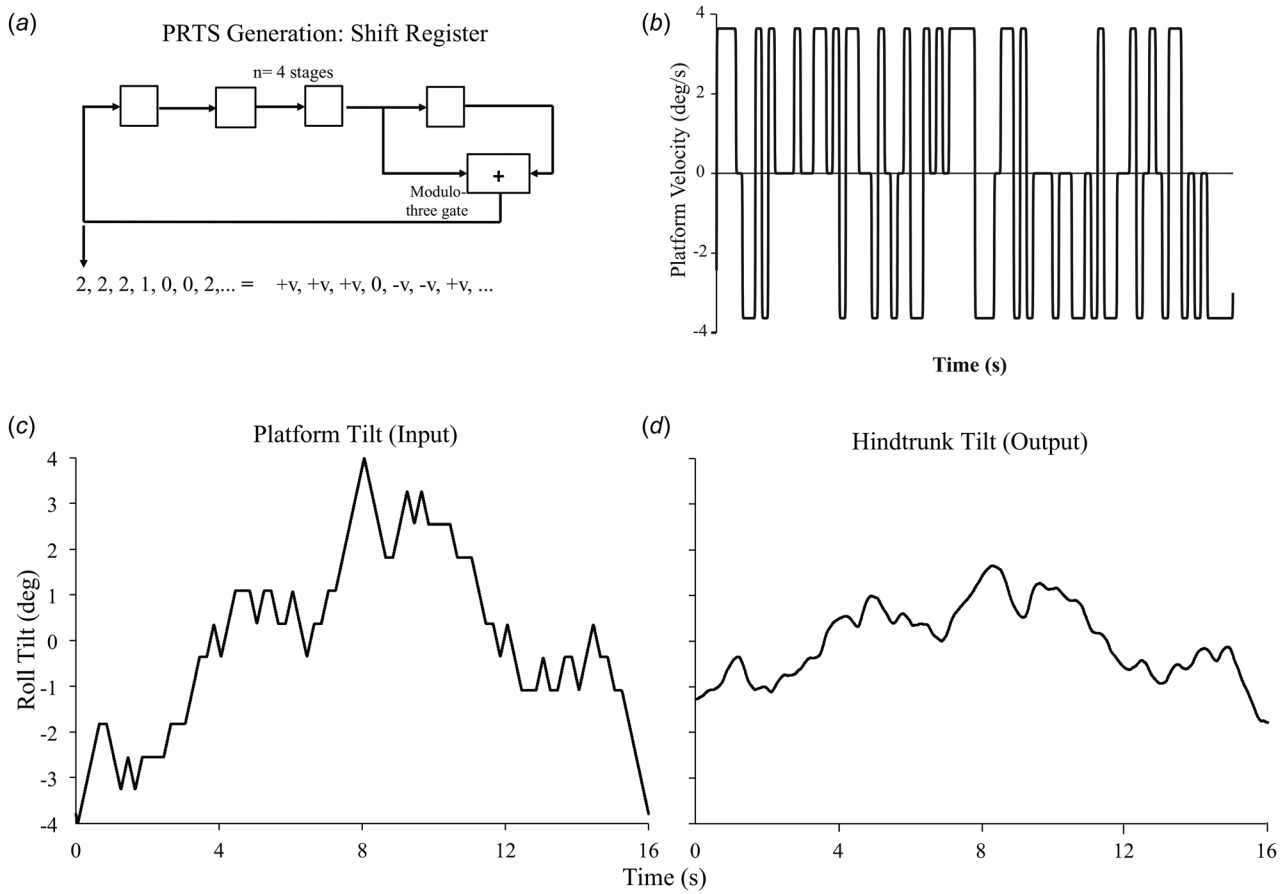

Fig. 1 Schematic of PRTS generation and application

Equations (5)–(7) show magnitude and phase of the transfer function, as well as coherence, respectively

$$tf_{\text{exp.gain}} = |H(\omega)| = \sqrt{H(j\omega)^* \cdot H(j\omega)} \tag{5}$$

$$tf_{\text{exp.phase}} = \angle H(\omega) = \left(\frac{180\,\text{deg}}{\pi}\right)\tan^{-1}\left(\frac{\text{Im}(H(j\omega))}{\text{Re}(H(j\omega))}\right) \tag{6}$$

$$\gamma^2(\omega) = \frac{|G_{xys}(j\omega)|^2}{G_{xs}(\omega) \cdot G_{ys}(\omega)} \tag{7}$$

As described above (in Eqs. (6) and (7)), transfer function gain and phase were computed from the measured trunk roll-tilt and PRTS roll-tilt stimulus. All computations were conducted in MATLAB (MathWorks, Natick, MA, version 2008b).

Significance of Gain, Phase, and Coherence. Here, we overview the significance of the gain and phase values. Trunk sway was calculated with respect to earth vertical; a gain = 0 indicates that the trunk orientation is stable relative to earth vertical. Conversely, if gain = 1 at a particular frequency, this indicates that the trunk orientation is stable relative to the platform surface (i.e., trunk sway equals platform tilt angle) at that particular frequency. If the gain > 1, then the trunk tilt is larger than the platform tilt. A phase = 0 deg at a particular frequency indicates that the motion of the trunk is synchronous with the platform tilt stimulus at that particular frequency. However, a phase <0 deg or phase >0 deg means that the motion of the trunk is either lagging or leading the platform stimulus, respectively.

In order to determine system linearity and noise between the stimulus and response, coherence functions were computed. Coherence can vary from 0 to 1, with 1 indicating a perfect linear correlation between stimulus and response when no noise is present; and 0 indicating that there is no linear correlation between stimulus and response or extreme noise.

Feedback Controller Model. Transfer functions derived from the measured data were used in conjunction with a sensorimotor integration model. This model, previously used in numerous human studies (referenced above), was used here to test the sensory reweighting hypothesis for the rhesus monkey hindtrunk. In particular, the model was implemented to determine if changes in model parameters (e.g., sensory weights) across stimulus amplitudes and also between normal and mBVH sensory states could predict the measured hindtrunk results. The model implemented is shown in Fig. 2 and described by Eq. (8).

For a pseudorandom roll-tilt input, the support surface input is the roll-tilt waveform itself, and the monkey's hindtrunk sway (HS) is the output response. For quiet stance or small platform motions, some models of bipedal human stance have treated the human as a single-link inverted pendulum that is inherently unstable. Because the platform underwent only small perturbations, we modeled the rhesus monkey's bipedal hindtrunk as an inverted pendulum. When there is deviation from upright stance, a corrective torque (T_c) comprised of the summation of an intrinsic/short-latency torque (T_p), generated by mechanisms without time delay (or with short time delay) and a torque (T_a) generated by mechanisms with long-latency neural time delay. The torque (T_p), is generated by the inherent mechanical characteristics of the muscles, joints, ligaments, and musculoskeletal system (time delay = 0) and short-latency reflexes. The intrinsic/short-latency mechanisms consist of stiffness and damping (K and B, respectively). In order to stabilize the pendulum body, a long-latency

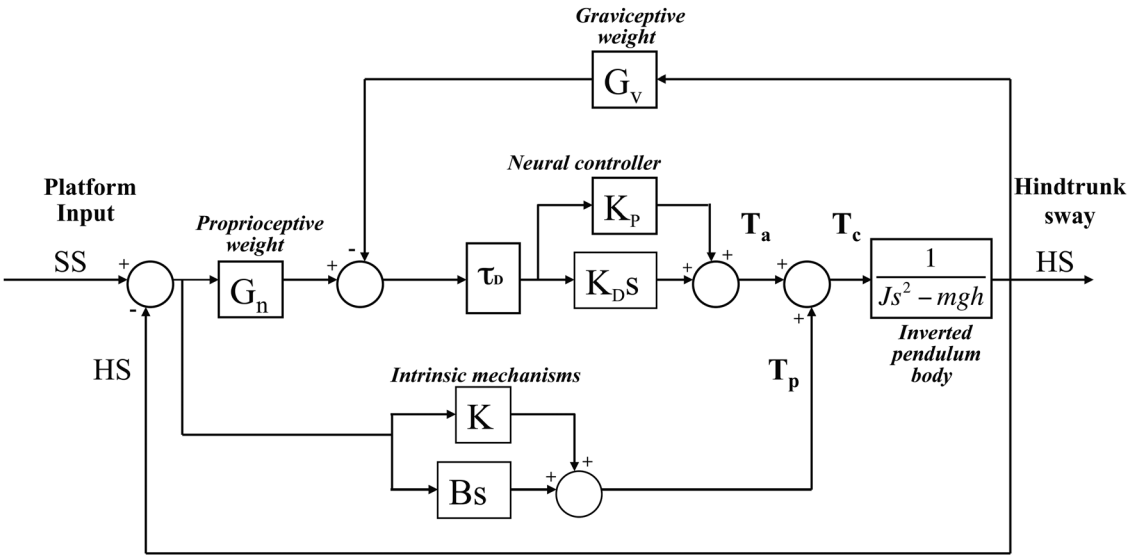

Fig. 2 Modified sensory integration feedback controller model for the rhesus monkey hindtrunk

(~200 ms [10]) torque (T_a) requires a corrective torque equal to the angular deviation times the long-latency stiffness represented by K_P, where "P" indicates proportional feedback, and another component that is the time derivative of the angular deviation times the long-latency damping represented by K_D, where "D" indicates derivative feedback. This long-latency torque is based on sensory feedback. The weights of sensory channels, proprioceptive (G_n) and graviceptive (G_v), were assumed to sum to unity. Since all experiments were conducted in dim lighting with a black tarp surround to limit visual cues, the visual weight was assumed to be ~0.

In modeling the rhesus hindtrunk, the moment of inertia of the hindtrunk ($J = 0.09\,\text{kg*m}^2$) and hindtrunk mass × gravity × hindtrunk COM height ($\text{mgh} = 2.054\,\text{kg*m}^2/\text{s}^2$) were determined using anthropometric measurements derived from cadaveric rhesus monkeys [21]. Transfer functions derived from the empirical results were used in conjunction with transfer functions derived from the modified independent channel model (8) to determine model parameters that minimized the normalized-mean-square-error (described in Eq. (10)). Within Eq. (8), tf_{model} (or HS/SS) is the transfer function of output hindtrunk roll/input platform tilt, s is a complex variable, K_P is the proportional gain or "long-latency stiffness," K_D is the derivative gain or "long-latency damping", τ_D is the long-latency time delay, G_n is the proprioceptive gain, and G_v is the vestibular gain (which will sum to Eq. (1)), K is the intrinsic/short-latency stiffness, and B is the intrinsic/short-latency damping

$$tf_{\text{model}} = \frac{\text{HS}(s)}{\text{SS}(s)} = \frac{(Bs + K) + G_n(K_D s + K_P)e^{-\tau_D s}}{(Bs + K) + Js^2 - \text{mgh} + (K_D s + K_P)e^{-\tau_D s}} \tag{8}$$

Model Parameter Estimation. By estimating model parameters, we determined if changes in empirical posture dynamics across stimulus amplitude and between normal versus mBVH states were due to sensory reweighting or changes in other neural processes such as stiffness, damping, or sensorimotor integration time delays. To estimate parameters, first, model transfer functions were compared to the empirical (experimental) transfer functions, tf_{exp}, computed from measured roll data and, tf_{model}, transfer function computed by model to estimate the error, E, shown in Eq. (9). The error, E, is the difference between the model and empirical transfer functions divided by the magnitude of the model transfer function. This definition of E was determined heuristically in previous human studies (e.g., Refs. [8–10,12], and [22]) to obtain quality and meaningful model fits to transfer functions derived from the measured human data. A constrained optimization function ("fmincon," MATLAB Optimization Toolbox) was used to adjust the model parameters to minimize the normalized mean square error described in Eq. (10). The NMSE is the mean of the error times the conjugate of the error

$$E = \frac{tf_{\text{exp}} - tf_{\text{model}}}{|tf_{\text{model}}|} \tag{9}$$

$$\text{NMSE} = \text{mean}(E \bullet E^*) \tag{10}$$

Model parameter estimates were determined for the 1, 4, and 8 deg pp normal and mBVH data. For each of the 1, 4, and 8 deg pp PRTS stimulus amplitudes, a set of optimized model parameters was computed from the measured data, and the NMSE was computed as shown in Eq. (10) for each individual PRTS amplitude. However, we also estimated model parameters for all stimulus amplitudes using *simultaneous* model parameter estimation involved. This involved the constraint of specific model parameters to be equal across the 1, 4, and 8 deg pp stimulus amplitudes and a normalized-mean-square-error was the sum of the error terms for the 1, 4, and 8 deg pp PRTS stimulus amplitudes. For the simultaneous parameter estimation, we will call the normalized-mean-square-error term "NMSE_{sim}" to differentiate from "NMSE."

Results

Foretrunk and Hindtrunk Stimulus–Response Curves. Foretrunk and hindtrunk RMS roll as a function of stimulus amplitude (stimulus–response curves) are shown in Fig. 3. In Fig. 3, the dotted lines in each represent the foretrunk or hindtrunk RMS roll for the zero stimulus amplitude (or a stationary platform). For the normal animal's foretrunk, the stimulus–response curve was roughly flat for the three lowest and two highest stimulus amplitudes. For roll-tilts < 4 deg pp, the normal animal's foretrunk was not responding to the stimulus in that RMS roll was comparable to values seen for no platform motion (i.e., quiet-standing). The types of saturation seen in stimulus–response curves of the foretrunk and hindtrunk were different, which implied that there were different mechanisms involved in the control of the foretrunk or hindtrunk (see Discussion). However, for the normal animal's hindtrunk stimulus–response curve, there was a visible

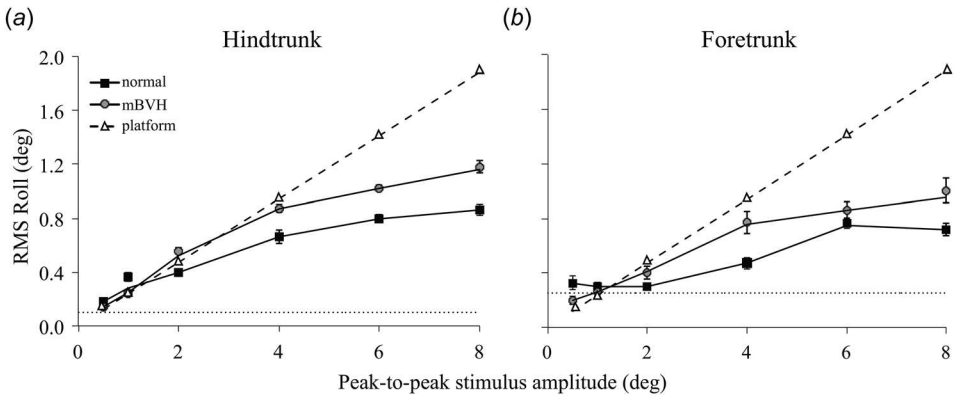

Fig. 3 (*a*) RMS roll of hindtrunk and (*b*) foretrunk as a function of stimulus amplitude with standard error bars. Black-dotted lines represent foretrunk or hindtrunk RMS roll value for stationary platform (i.e., quiet-standing). Normal data: 18 cycles per amplitude; mBVH: 23 cycles per amplitude.

nonproportional increase in RMS roll, or sway saturation, at the higher amplitudes that was also seen in normal humans [10].

For the animal in the mBVH state, the hindtrunk stimulus–response curve showed that the RMS roll saturates at the larger stimulus amplitudes but to a lesser extent than in the normal state. When compared to the normal response, the hindtrunk stimulus–response curve for the mBVH state showed a slight decrease or no significant difference at the lowest stimulus amplitudes but was elevated at the larger stimulus amplitudes. For both normal and mBVH states, the hindtrunk was clearly showing sway saturation.

Foretrunk Transfer Functions. For 1–8 deg pp stimulus amplitudes, normal foretrunk transfer function gain was < 1 and approximately constant across frequency (Fig. 4(*a*)). For all stimulus amplitudes, foretrunk phase (Fig. 4(*c*)) had ~0 lag (i.e., foretrunk was in phase with the platform) at the lowest frequencies, then increased in phase lag with increasing stimulus frequency. Furthermore, foretrunk coherence (Fig. 4(*e*)) was low ($<\sim 0.6$) for all stimulus amplitudes, except for the 6 and 8 deg pp amplitudes at low frequencies, indicating that, in general, any relationship between the stimulus and the foretrunk roll was weak.

In the mBVH animal, foretrunk transfer function gain was relatively flat across stimulus amplitudes and frequencies (Fig. 4(*b*)) and in some cases less than normal (e.g., at the lowest frequency for the 1 and 4 deg pp stimuli). The animal in the mBVH state had a slight phase lead for the lowest stimulus frequency (i.e., foretrunk was leading the platform stimulus) compared to the normal animal for the 1 and 4 deg pp stimuli. Given that the lowest stimulus frequency for the 1 and 4 deg pp stimuli had a ~0 coherence, it was not surprising that the gain and phase were very different compared to the other frequencies. As seen in the normal animal, the mBVH foretrunk response phase lag increased with increases in frequency (Fig. 4(*d*)). The mBVH coherence (Fig. 4(*f*)) was $<\sim 0.6$ for all stimulus amplitudes and was the smallest for the lowest stimulus frequency in the 1 and 4 deg pp responses (i.e., ~0 coherence), indicating a weak relationship between the stimulus and foretrunk roll.

Hindtrunk Transfer Functions. In the normal hindtrunk transfer function gain (Fig. 5(*a*)), sway saturation was seen in that the gain tended to decrease away from 1 as stimulus amplitude increased. However, for the lower amplitudes, normal hindtrunk gains were ~1 indicating that the animal was orienting more with the platform. Hindtrunk gain for lower stimulus amplitudes (i.e., 1 and 2 deg pp) at frequencies up to 1 Hz were slightly >1, which means that hindtrunk roll was slightly greater than that of the platform. For larger stimulus amplitudes (i.e., 6 and 8 deg pp), the gain was <1 for all frequencies consistent with hindtrunk roll saturating at larger amplitudes (shown in Fig. 5(*a*)). For neither normal nor mBVH states were resonant peaks observed. For larger stimulus amplitudes, this shift away from a gain $= 1$ (toward gain $= 0$) indicated that the hindtrunk was aligning increasingly more with earth-vertical and less with the platform surface. For all stimulus amplitudes, hindtrunk phase showed ~0 lag at the lowest frequencies, and increased phase lag for increased frequency (Fig. 5(*b*)). In general, mBVH hindtrunk coherence (Fig. 5(*f*)) was higher than normal foretrunk coherence at the lowest frequencies (Fig. 5(*e*)) and decreased in coherence as the stimulus frequency increased.

For the mBVH hindtrunk transfer function gains (Fig. 5(*b*)), most gain functions were elevated relative to the normal gains. For example, for the lowest frequency (0.0625 Hz) with the highest coherence, mBVH gain was significantly greater than normal at all amplitudes greater than 1 deg pp (2 deg pp: $\mathrm{df} = 30$, $t = 6.829$, $p < 0.001$; 4 deg pp: $\mathrm{df} = 12$, $t = 3.876$, $p < 0.005$; 6 deg pp: $\mathrm{df} = 18$, $t = 3.239$, $p < 0.005$; 8 deg pp: $\mathrm{df} = 36$, $t = 4.119$, $p < 0.001$). For all stimulus amplitudes, hindtrunk phase (Fig. 5(*d*)) showed ~0 phase lag at the lowest frequencies, then increasing phase lag with increasing stimulus frequency. The mBVH hindtrunk coherence (Fig. 5(*f*)) was generally higher than normal foretrunk coherence for frequencies <0.3 Hz indicating a more linear relationship between the platform tilt stimulus and hindtrunk response at the lower frequencies. As in the normal hindtrunk response, coherence decreased substantially at higher frequencies.

Posture Modeling to Describe Sensorimotor Integration

Exploration of Frequency Bands and Intrinsic Parameters. We investigated the model across three frequency ranges (0.0625–2.33 Hz, 0.0625–1.125 Hz, and 0.0625–0.625 Hz) using: (1) a "basic model" that included long-latency (neural controller) stiffness (K_P) and damping (K_D), sensory weight (G_n), and long-latency time delay (τ_D); and (2) the basic model (consisting of K_P, K_D, G_n, and τ_D) with the addition of model parameters for intrinsic/short-latency stiffness (K) and damping (B). Eq. (10) was the metric used to assess the degree to which the model-derived transfer functions predicted those computed from measured data. We found that model fits were not possible for the ranges of 0.0625–2.33 Hz (the full frequency range) or 0.0625–1.125 Hz as NMSEs were too high (e.g., NMSE > 0.4). This was due to: (1) intrasubject variance and (2) low coherence at the higher frequencies. We therefore restricted the parameter estimation procedure to the lower input spectrum of 0.0625–0.625 Hz because coherence was relatively high across this range.

In addition, we found that including intrinsic/short-latency model parameters K and B was not suitable to an interpretable model. While their inclusion could reduce the NMSE, it led to

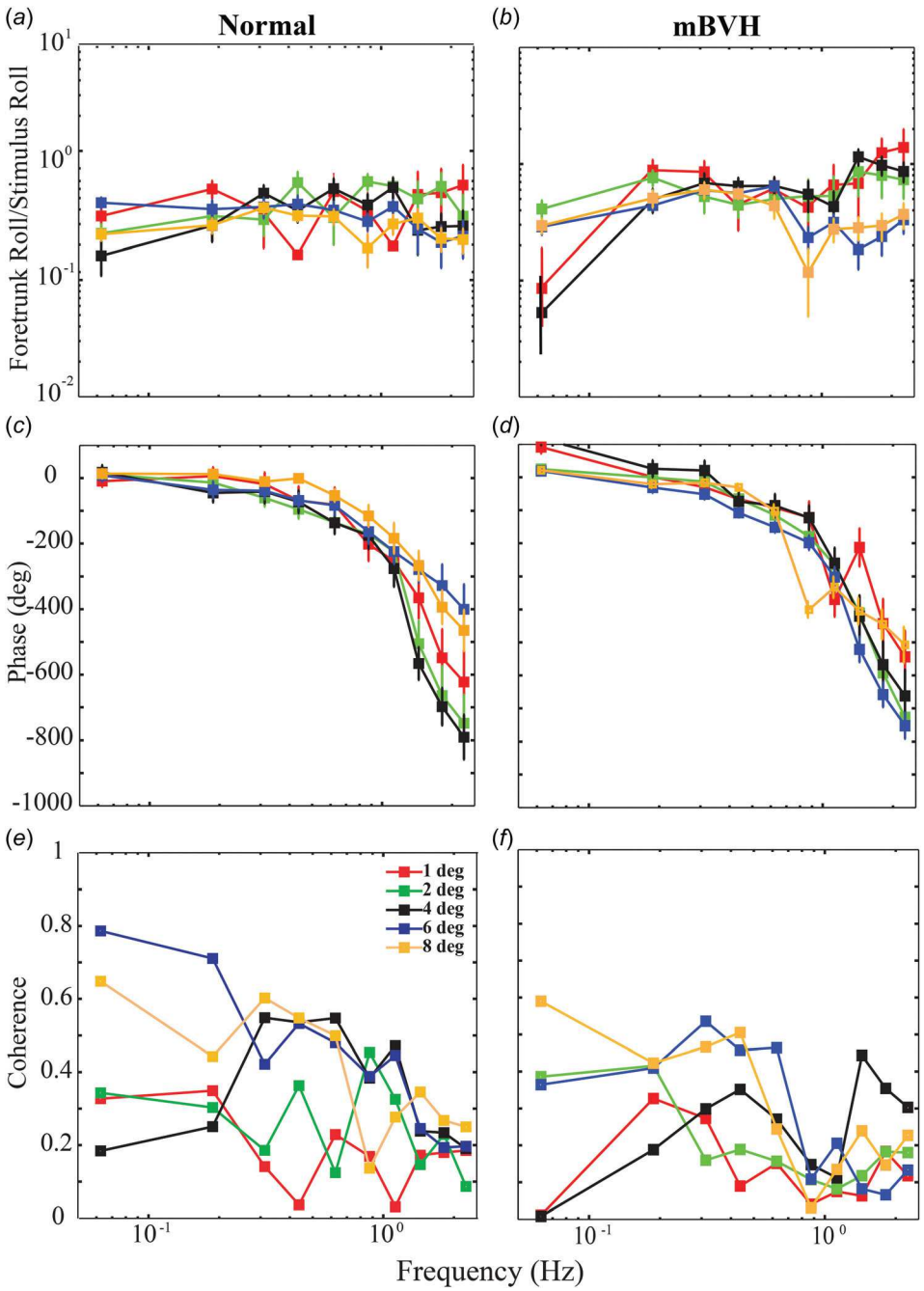

Fig. 4 Foretrunk transfer function gain, phase, and coherence for normal ((*a*), (*c*), (*e*)) and mBVH ((*b*), (*d*), (*f*)) sensory states. Bars shown represent standard error. Normal data: 18 cycles per amplitude; mBVH: 23 cycles per amplitude.

unrealistic increases and decreases in parameters with no clear pattern across stimulus amplitudes; this was most likely due to too many free parameters. Since relatively large values of intrinsic/short-latency parameters (e.g., a relatively large value of intrinsic/short-latency stiffness, K) and proprioceptive weighting, G_n, (e.g., $\sim$1) results in orientation to the platform surface, these two parameters were redundant within the model. Furthermore, inclusion of the intrinsic/short-latency parameters, K and B, led to unrealistically large time delays (τ_D). For example, for the mBVH 8 deg pp condition, a model-estimated time delay was $\sim$646 ms, much longer than the physiologic time delays of 170–200 ms reported for humans [10].

Sensory Reweighting and Parameter Variations. Figure 6 shows overlaid plots of the model and empirical fits for normal and mBVH states, respectively, and Fig. 7 shows the model parameter estimates computed from the hindtrunk results measured at the 1, 4, and 8 deg pp stimulus amplitudes. Figure 7 displays that the animal in the normal state weighted graviceptive (e.g., vestibular) cues more heavily than proprioceptive cues as stimulus amplitude increased. In the mBVH state, the trend toward increased vestibular weight across stimulus amplitude was less evident. At the 4 and 8 deg pp amplitudes, the vestibular weight in the mBVH was lower than the normal state. These results are consistent with the stimulus–response and hindtrunk transfer function (Figs. 3 and 5, respectively) results that show that the normal animal oriented its hindtrunk more with earth-vertical than the support surface at the larger stimulus amplitudes, leading to sway saturation, and that the animal in the mBVH state oriented its hindtrunk more with the platform surface than earth-

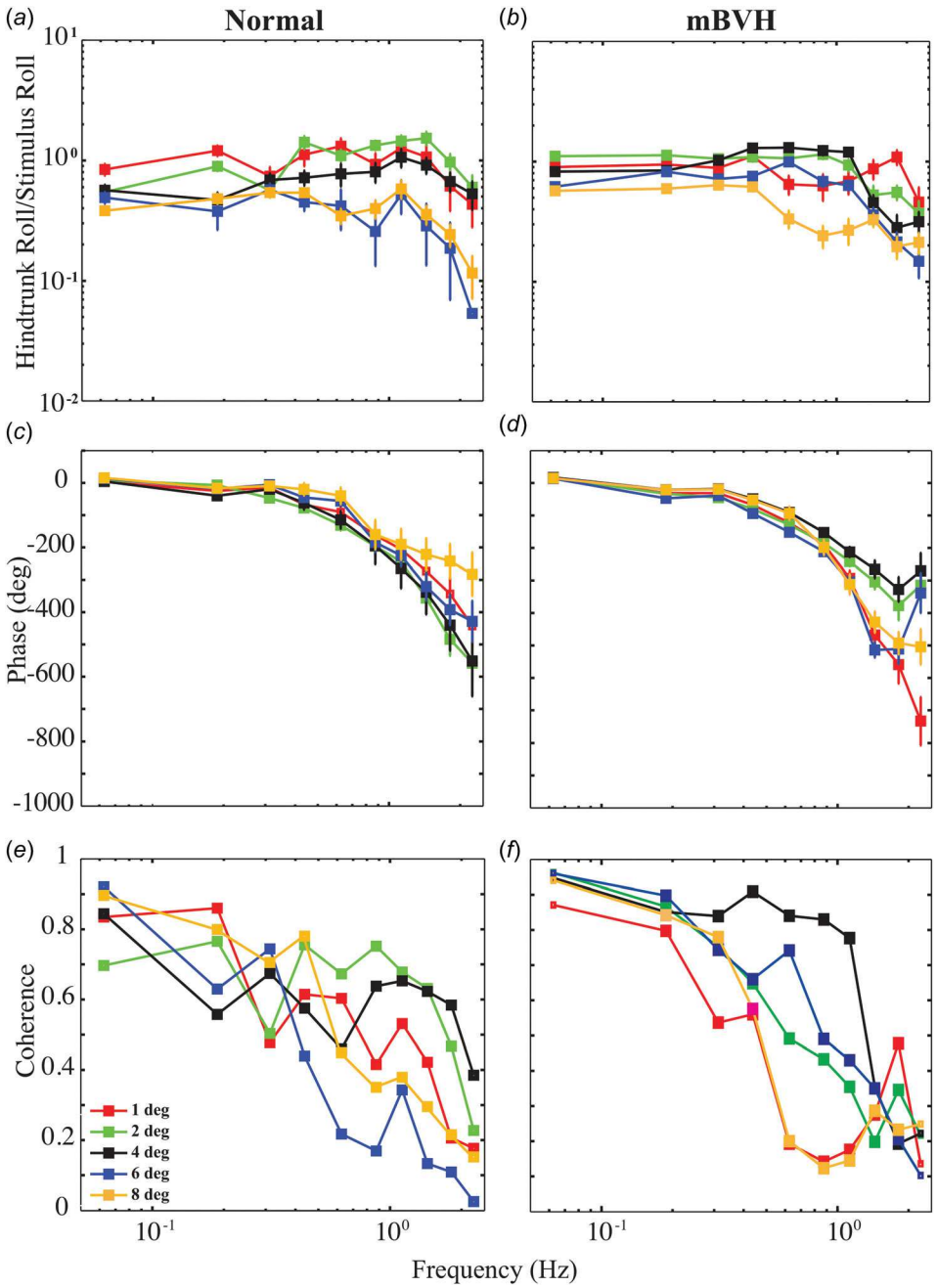

Fig. 5 Hindtrunk transfer function gain, phase, and coherence for normal ((*a*), (*c*), (*e*)) and mBVH ((*b*), (*d*), (*f*)) sensory states. Bars shown represent standard error. Normal data: 18 cycles per amplitude; mBVH: 23 cycles per amplitude.

vertical at the higher stimulus amplitudes, leading to increased roll compared to normal. In the normal state, long-latency (neural controller) damping, K_D, increased for the largest stimulus amplitude; however, long-latency (neural controller) stiffness, K_P, showed little change across stimulus amplitudes. Increases in K_D may increase the stability of the system, reduce the overshoot, and improve the transient response [23]. Here, we deduced that the increase seen in K_D in the normal animal for the largest stimulus amplitude caused reduction in the (output) hindtrunk RMS roll (Fig. 3) and frequency response gain (Fig. 5). Time delay, τ_D, also increased for the largest stimulus amplitude; however, this may have been due to the correlation ($R^2 = .9823$) of K_D and τ_D within the model as opposed to physiologic changes in τ_D.

In the mBVH state, K_P increased with stimulus amplitude, whereas in the normal state, K_P remained relatively constant. It had been observed previously that severe bilateral vestibular-loss human subjects had increases in long-latency (neural controller) stiffness in comparison to normal test subjects and hypothesized that this could serve as a compensation mechanism [10]. Increases in K_P are known to decrease the rise time but increase the overshoot of the response [23]. Therefore, increases in stiffness without increases in damping could yield a more oscillatory response and increased gains (e.g., in the mBVH animal, K_P increased with stimulus amplitude).

To understand which model parameter had the largest explanatory power in accounting for the changes in posture across stimulus amplitude, we performed additional fits where one parameter was fixed across stimulus amplitude during the fitting. Figure 8 shows NMSE_{sim} on the y-axis as a function of the fixed model parameters on the x-axis for the normal sensory state.

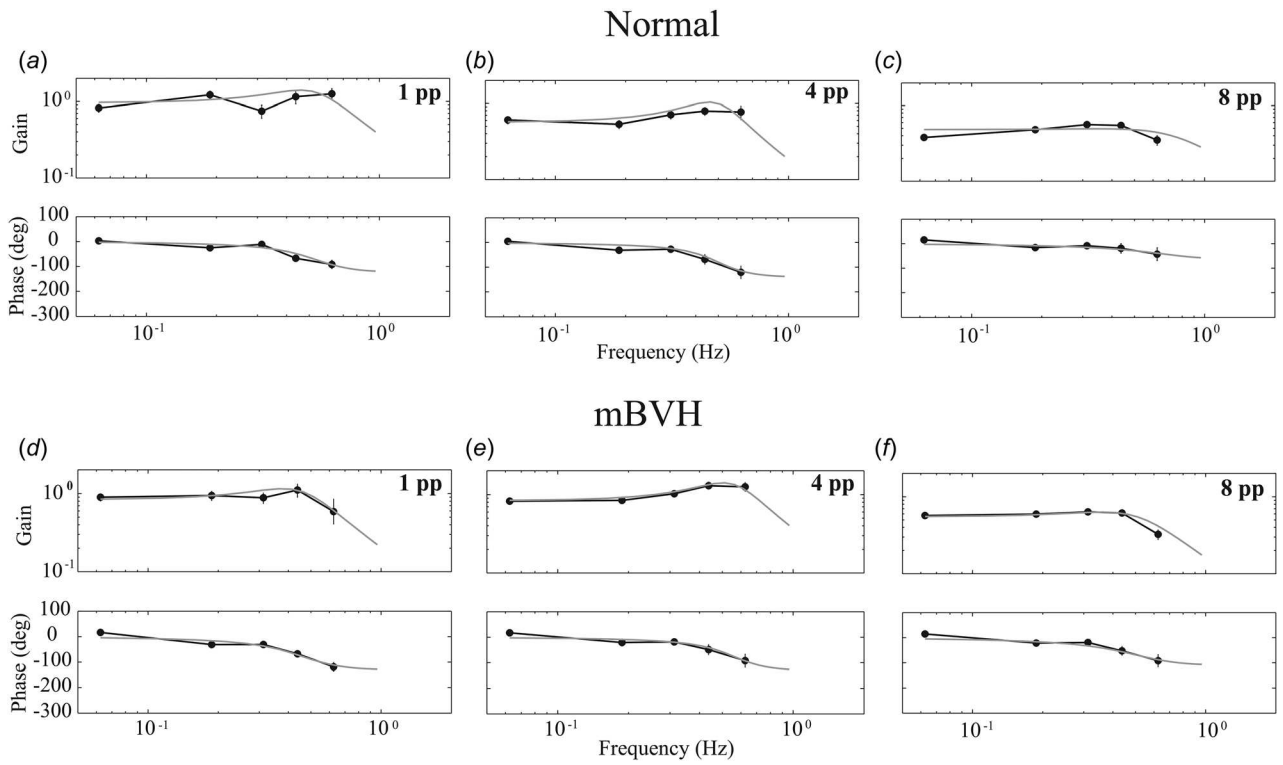

Fig. 6 Model (gray) and measured (black) hindtrunk transfer functions with standard error bars for the normal sensory state ((*a*)–(*c*)) mBVH sensory state ((*d*)–(*f*))

When the individual model parameters τ_D, K_D, and K_P were constrained across stimulus amplitude, there was little change in $NMSE_{sim}$, suggesting that allowing all of these parameters to vary added redundancy to the model and the monkey. However, when the sensory weight (G_n) was constrained (held constant) across stimulus amplitude, there was an increase in $NMSE_{sim}$, for the normal sensory state (Fig. 8). Because of the importance of G_n varying across stimulus amplitude, we also examined if the sensory weight alone could explain all the changes seen in the 1, 4, and 8 deg pp normal measured transfer functions. We examined this by allowing only sensory weight, G_n, to vary across stimulus amplitude and constrained all other model parameters to be equal across stimulus amplitude. However, this model iteration resulted in an $NMSE_{sim}$ of 0.42, leading us to the conclusion that other variation in parameters, in addition to sensory weight, were needed across stimulus amplitude to fully account for the empirical results.

Discussion

Here, we describe the interpretation of our results for normal and mBVH primate responses (the first of their kind) and the model results from the use of system identification techniques and a feedback controller model previously only applied for the study of human postural responses. From our model, we were able to determine meaningful parameters that describe a neurophysiological basis for balance for different levels of vestibular function.

Our observation that rhesus macaques and humans have even remotely similar postural control motivates further application of the rhesus macaque as a model for studying vestibular dysfunction's effects on human postural control. The normal monkey's hindtrunk stimulus–response and transfer results showed characteristics similar to those seen in humans. Specifically, (hindtrunk) sway saturation for increasing stimulus amplitude was observed. From the hindtrunk stimulus–response and transfer function results, it was hypothesized that sway saturation was caused by the normal rhesus monkey's increased weighting of its graviceptive cues for larger stimulus amplitudes (sensory reweighting) to limit the roll of the trunk. A feedback controller model, previously only applied to human postural control, was modified and implemented to test the sensory reweighting hypothesis in a normal and mild vestibular-impaired primate. Our modeling observations not only confirmed our hypothesis, but also confirmed that sensory reweighting could exist in animals other than humans (rhesus monkeys).

Sensory Reweighting Seen in Hindtrunk but Not Foretrunk. Empirical characteristics associated with sensory reweighting (saturation) were apparent in the normal hindtrunk response to the platform stimulus, but not the foretrunk (Figs. 3–5). One reason for this may be due to different mechanical functions of the foretrunk and hindtrunk. In quadrupeds, it has been proposed that the foretrunk is used primarily to provide stability as struts that stiffen, support, and help steer the animal [24]; however, the hindtrunk is used to generate propulsive forces [25] and therefore the postural control mechanisms associated with each are likely to differ. In normal humans, a previous study characterized sensorimotor integration in the frontal plane and described the upper body and lower body utilizing different control mechanisms [22]. The lower body control relied primarily on sensory feedback and control mechanisms across stimulus amplitude that was consistent with sensory reweighting (i.e., amplitude-dependent reliance predominantly on proprioceptive or graviceptive cues). In upper body control, sensory reweighting was not the dominant mechanism, but instead, intrinsic/short-latency musculoskeletal mechanisms along with a relatively fixed reliance on sensory feedback across stimulus amplitudes.

Our study was based on a single test subject and therefore we cannot generalize. However, based on our observed results (i.e., stimulus–response curves and transfer functions) shown here, we proposed that: (1) the foretrunk may be utilizing a different mechanism for control (i.e., not predominantly utilizing the sensory-mediated mechanisms, such as sensory reweighting) and (2) the hindtrunk may be predominantly utilizing sensory

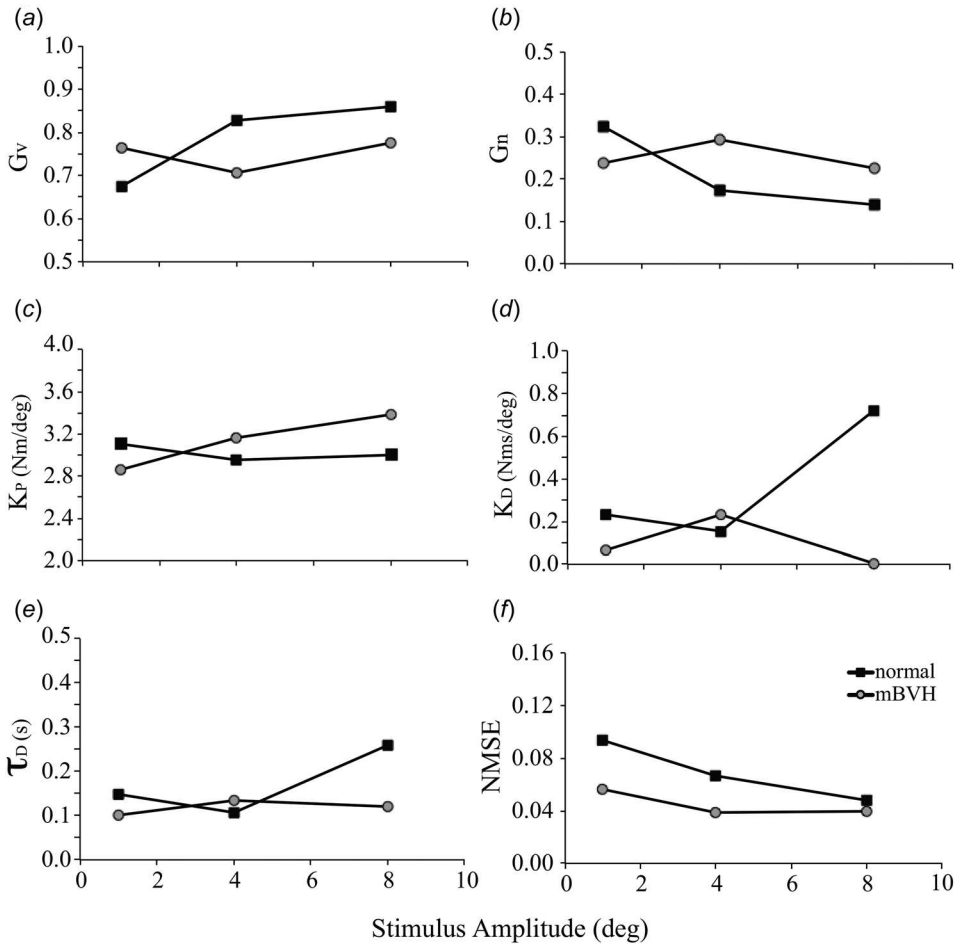

Fig. 7 Nonsimultaneous model parameter estimates ((*a*)–(*e*)) and NMSE (*f*) as a function of stimulus amplitude for the normal (black squares) and mBVH (gray circles) sensory states

feedback, thus leading to a saturating response seen in both the stimulus–response and transfer function gains of the normal and mBVH states. In this paper, we focused on sensory reweighting in the animal's hindtrunk. We therefore focused our model on the hindtrunk only, but may explore foretrunk postural control in future work.

Modeling to Describe Sensory Reweighting. The goal of our modeling was to adapt and build on models previously only applied to human posture and to capture the meaningful characteristics (via physiologic model parameter estimates) of rhesus monkey posture.

The modeling results (Figs. 7(*a*), 7(*b*), and 8) were consistent with sensory reweighting being present in the normal state. Specifically, as stimulus amplitude increased, the monkey increased reliance on vestibular cues and decreased reliance on proprioceptive cue. Moreover, when the individual model parameters τ_D, K_D, and K_P were constrained across stimulus amplitude, there was little change in $NMSE_{sim}$, suggesting that allowing these parameters to vary added redundancy to the model. However, when the sensory weight (G_n) was constrained (held constant) across stimulus amplitude, there was an increase in $NMSE_{sim}$, for the normal sensory state (Fig. 8), suggesting that changes in the sensory weight are needed for the model to describe the empirical data and that the nervous system may in fact primarily modulate the sensory weight across stimulus amplitude. Despite the importance of sensory weights changing across stimulus amplitude and sensory state, our results do imply that the animal modulated other neural control parameters, as described in Fig. 7.

Only limited human posture data exist for vision-limited, pseudorandom support surface tilt conditions, and there is no such previously published posture data from primates. Direct comparisons between the magnitudes for K_P and K_D in the rhesus versus human were challenging. For the rhesus monkey, it was observed that both K_P and K_D were much smaller in magnitude than observed in normal humans, for similar test conditions [10]. These differences are likely due to the fact that the rhesus macaque is much shorter in height and has much less mass than humans. It had been previously shown that there is a positive correlation between mass and

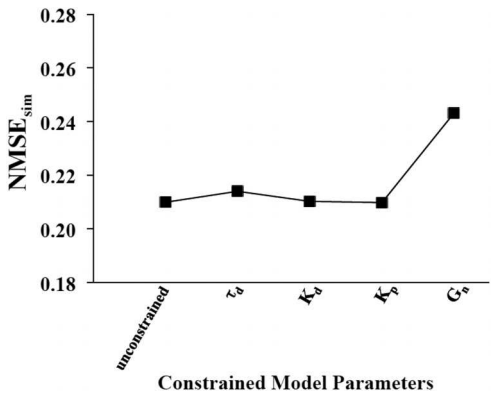

Fig. 8 $NMSE_{sim}$ for the normal state as a function of constrained model variation

center-of-mass height for both K_P and K_D [10]. However, extrapolation proved difficult, and likely inaccurate, in this case in that human mass and height are distinctly larger and heavier than rhesus macaques. An observable and perhaps the most important consistency for both normal humans and normal rhesus monkey were that they show observed decreases in proprioceptive weighting and increases in graviceptive weighting as platform stimulus amplitude increased. Moreover, in humans, the ratio of stiffness, K_P, to the minimum stiffness required to resist gravity (mass $\times$ g $\times$ center of mass height) was on average 1.3. In our study, we found a very similar ratio of 1.4 to 1.5 across normal state test conditions. Also, the ratio of damping K_D to K_P was fairly similar between humans ($\sim$33%) and our monkey study (9–38%). Furthermore, the time delays were similar between humans and those observed our study.

Animal Models: Larger Goals. We are aiming for our work to serve as a basis for a larger empirical framework targeting the characterization of invasive prototype prostheses aimed toward restoring balance, and preventing falls, in vestibular-impaired humans. This was the first-ever attempt at modeling monkey postural responses and determining physiologic model parameters to account for the observed empirical behaviors. By establishing a systems identification approach, it is possible to quantify sensory contributions and neural adaptations that occur at various stages of vestibular function and to quantitatively assess if and how nonhuman primates incorporate a vestibular prosthesis.

Our long-term goal is to utilize a primate model that accurately captures underlying neural characteristics of prostheses that improve balance. The work described here will assist in the quantification of target therapies and treatment response, in particular, to rehabilitative therapies that cannot yet be applied to humans and proof of concept (in nonhuman primates) is necessary as a precursor.

Conclusions

Our analysis of normal monkey postural responses to pseudorandom tilts showed similarities to that of human responses. Rhesus monkey hindtrunk RMS roll as a function of pseudorandom roll-tilt amplitude (i.e., stimulus–response curves) showed striking similarity to those seen in normal humans [10] in that the hindtrunk sway generally followed the platform tilt waveform, remained relatively constant across repeated cycles, contained power primarily at the stimulated frequencies, and saturated with increases in stimulus amplitude. Through characterization of stimulus–response curves, transfer function analysis, and modeling techniques, we found results were from a nonhuman primate were consistent with the sensory reweighting hypothesis in that: (1) the normal model parameter results were showed evidence of greater weighting of graviceptive cues (and decreased weighting of proprioceptive cues) at larger platform tilts and (2) the model parameter results for the mildly impaired state showed that graviceptive weighting increased with platform tilt, but not to the extent seen in the normal state. Consistent with the mild vestibular impairment, the mBVH model predicted less sensory reweighting than in the normal state. The model fitting to the mBVH data exemplifies that the model can detect more subtle changes in sensory reliance (e.g., normal function versus mild vestibular impairment).

In summary, our results show that a sensory integration model previously only used to describe human posture can be applied to the bipedal hindtrunk of a nonhuman primate, and that the sensory integration model is sensitive enough to capture sensory weighting differences for even mild levels vestibular dysfunction. These findings are encouraging in that animals, such as rhesus monkeys, could be used for future posture studies involving the development of invasive prostheses and rehabilitative methods that are not yet ready for human trials.

Acknowledgment

We thank Dr. Conrad Wall for advice on empirical design and James Lackner.

Funding Data

- National Institutes of Health (NIH) (Grant Nos. DC8362 and T32 DC00038).
- National Science Foundation (NSF) (Grant Nos. 1533479, 1700219, and 1654474).

Appendix

Pseudorandom noise signals [20] can have a number of output states (e.g., binary (or two output states), ternary (or three output states), and pentary (or five output states)) depending on the application. A pseudorandom ternary sequence, or PRTS (depicted in the schematic of Fig. 1, top), can be generated using a shift register and consists of 3 output states: 0, 1, and 2. In applying a PRTS input stimulus to the balance platform, 0 corresponded to negative platform velocity (or "$-v$"), 1 corresponded to zero platform velocity, and two corresponded to positive platform velocity (or "$+v$").

The sequence is initialized with a series of logics states. Within the shift register, each stage is cross-connected and simultaneously triggered by a clock pulse, or the shift time (Δt). For each clock pulse, the logic contents of the ith stage are transferred to the $(i+1)$st stage and a new logic state is introduced to the input of the first stage via the feedback circuit. The sequence obtained from the shift register depends on where the feedback connection is inserted. A modulo-three gate produces the sum-digit result the same as regular addition.

A maximum length sequence, described in Eq. (A1), is one in which the length of the pseudorandom sequence, N, is maximum for the given number of stages within the register, n, before the sequence repeats itself. For a ternary sequence, there are a total of 3^n different states; however, occurrence of the state in which the shift register contains 0 logic in each of its stages (meaning all zero sequence) must be prevented. Thus, the largest possible length, N, is the following:

$$N = 3^n - 1 \tag{A1}$$

The period of the pseudorandom ternary sequence, T, is described by Eq. (A2), where Δt is the shift time, and n is the number of stages.

$$T = \Delta t(3^n - 1) \tag{A2}$$

The frequency bandwidth Eq. (A3) of the sequence bounded by f_1 (lower frequency bound) and f_2 (upper frequency bound).

$$f_1 = \frac{1}{N\Delta t} \quad \text{to} \quad f_2 \cong \frac{1}{3\Delta t} \tag{A3}$$

For this study, a PRTS that operated using a four-stage shift register was used to generate an 80 length sequence. The selection of appropriate shift time and period was based on monkey's attention span and on the frequency bandwidth of interest. The animal tolerated a shift time of 200 ms, which yielded a cycle period of 16 s and a frequency bandwidth of 0.0625 to $\sim$2.33 Hz.

References

[1] Zapanta, P. E., Van Dusen, R., and DeVries, G. M., 2016, "Vestibular Rehabilitation," WebMD LLC, Atlanta, GA, accessed Oct. 16, 2017, http://emedicine.medscape.com/article/883878-overview

[2] Agrawal, Y., Carey, J. P., Della Santina, C. C., Schubert, M. C., and Minor, L. B., 2009, "Disorders of Balance and Vestibular Function in US Adults: Data From the National Health and Nutrition Examination Survey, 2001–2004," Arch. Intern Med., **169**(10), pp. 938–944.

[3] NIDCD, 2010, "Strategic Plan (FY 2006-2008)," National Institute on Deafness and Other Communication Disorders, Bethesda, MD, accessed May 20, 2010,

https://www.nidcd.nih.gov/sites/default/files/Documents/about/plans/strategic/strategic06-08.pdf
[4] American Speech-Language-Hearing Association, 2016, "More Than 1 in 20 U.S. Children May Have Dizziness, Balance Problems," ASHA Leader, **21**(4), p. 18.
[5] Horak, F. B., 2010, "Postural Compensation for Vestibular Loss and Implications for Rehabilitation," Restor. Neurol. Neurosci., **28**(1), pp. 57–68.
[6] Horak, F. B., and Macpherson, J. M., 1996, "Postural Orientation and Equilibrium," *Comprehensive Physiology*, American Physiological Society, Bethesda, MD, pp. 255–292.
[7] Thompson, L. A., Haburcakova, C. F., and Lewis, R. F., 2016, "Vestibular Ablation and a Semicircular Canal Prosthesis Affect Postural Stability During Head Turns," Exp. Brain Res., **234**(11), pp. 3245–3257.
[8] Goodworth, A. D., and Peterka, R. J., 2010, "Influence of Stance Width on Frontal Plane Postural Dynamics and Coordination in Human Balance Control," J. Neurophysiol., **104**(2), pp. 1103–1118.
[9] Goodworth, A. D., Wall, C., and Peterka, R. J., 2009, "Influence of Feedback Parameters on Performance of a Vibrotactile Balance Prosthesis," IEEE Trans. Neural Syst. Rehabil. Eng., **17**(4), pp. 397–408.
[10] Peterka, R. J., 2002, "Sensorimotor Integration in Human Postural Control," J. Neurophysiol., **88**(3), pp. 1097–1118.
[11] Camana, P. C., Hemami, H., and Stockwell, C. W., 1977, "Determination of Feedback for Human Postural Control Without Physical Intervention," J. Cybern., **7**(3–4), pp. 199–225.
[12] Cenciarini, M., Loughlin, P. J., Sparto, P. J., and Redfern, M. S., 2010, "Stiffness and Damping in Postural Control Increase With Age," IEEE Trans. Biomed. Eng., **57**(2), pp. 267–275.
[13] Johansson, R., and Magnusson, M., 1991, "Human Postural Dynamics," Crit. Rev. Biomed. Eng., **18**(6), pp. 413–437.
[14] Winter, D. A., 1995, "Human Balance and Posture Control During Standing and Walking," Gait Posture, **3**(4), pp. 193–214.
[15] van der Kooij, H., Jacobs, R., Koopman, B., and van der Helm, F., 2001, "An Adaptive Model of Sensory Integration in a Dynamic Environment Applied to Human Stance Control," Biol. Cybern., **84**(2), pp. 103–115.
[16] Macpherson, J. M., Everaert, D. G., Stapley, P. J., and Ting, L. H., 2007, "Bilateral Vestibular Loss in Cats Leads to Active Destabilization of Balance During Pitch and Roll Rotations of the Support Surface," J. Neurophysiol., **97**(6), pp. 4357–4367.
[17] Beloozerova, I. N., Zelenin, P. V., Popova, L. B., Orlovsky, G. N., Grillner, S., and Deliagina, T. G., 2003, "Postural Control in the Rabbit Maintaining Balance on the Tilting Platform," J. Neurophysiol., **90**(6), pp. 3783–3793.
[18] Brookhart, J. M., Parmeggiani, P. L., Petersen, W. A., and Stone, S. A., 1965, "Postural Stability in the Dog," Am. J. Physiol., **208**(6), pp. 1047–1057.
[19] Tukey, J. W., 1977, *Exploratory Data Analysis*, Addison-Wesley, Reading, MA.
[20] Davies, W. D. T., 1970, *System Identification for Self-Adaptive Control*, Wiley-Interscience, New York.
[21] Vilenksy, J. A., 1979, "Masses, Centers-of-Gravity, and Moments-of-Inertia of the Rhesus Monkey (Macaca Mulatta)," Am. J. Phys. Anthrop., **50**(1), pp. 57–66.
[22] Goodworth, A. D., and Peterka, R. J., 2012, "Sensorimotor Integration for Multisegmental Frontal Plane Balance Control in Humans," J. Neurophysiol., **107**(1), pp. 12–28.
[23] Ogata, K., 2003, *System Dynamics*, 4th ed., Prentice Hall, Upper Saddle River, NJ.
[24] Kimura, T., 1985, "Bipedal and Quadrupedal Walking of Primates: Comparative Dynamics," *Primate Morphophysiology, Locomotor Analyses Human Bipedalism*, University of Tokyo Press, Tokyo, Japan, pp. 81–104.
[25] Courtine, G., Roy, R. R., Hodgson, J., McKay, H., Raven, J. H., Zhong, H., Yang, M. H., Tuszynski, V., and Reggie Edgerton, 2005, "Kinematic and EMG Determinants in Quadrupedal Locomotion of a Non-Human Primate (Rhesus)," J. Neurophysiol., **93**(6), pp. 3127–3145.